

On tensor-product bases of PHT-spline spaces
Lisa Groiss, Bert Jüttler, Maodong Pan



On tensor-product bases of PHT-spline spaces

Lisa Groiss, Bert Jüttler and Maodong Pan

Abstract We show how to generate hierarchical T-meshes in \mathbb{R}^2 with associated locally refined B-splines, which possess the property of local linear independence, form a non-negative partition of unity, and span the resulting spaces of C^s -smooth polynomial splines of degree $p = 2s + 1$. The bases are collections of systems of tensor-product B-splines, without any need for truncation or similar modifications. The construction extends our earlier results for $s = 0$ and the bilinear case [12]. Additionally we introduce two new mesh quality parameters that control the local complexity and quality of the elements and show that these parameters are compatible with our mesh generation procedure. We also analyze their impact on the resulting meshes with the help of numerous examples. In order to make the paper self-contained, we also include a new proof (covering the case $p = 2s + 1$) of the fact – first noted by Dokken et al. [8] – that the resulting locally refined B-splines depend solely on the final mesh.

1 Introduction

Adaptive refinement of bivariate spline spaces plays an important role in geometric modeling and isogeometric analysis (IGA). It provides significant advantages over traditional NURBS techniques, which are based on a tensor-product structure that precludes local refinement. Several different approaches have been explored so far,

Lisa Groiss

Johannes Kepler University, Altenberger Straße 69, A-4040 Linz, e-mail: lisa.groiss@jku.at

Bert Jüttler

Johannes Kepler University and RICAM – Radon Institute for Computational and Applied Mathematics, Altenberger Straße 69, A-4040 Linz, e-mail: bert.juettler@jku.at

Maodong Pan

Nanjing University of Aeronautics and Astronautics, No. 29, Yudao Street, Nanjing, 210016, China, e-mail: mdpan@mail.ustc.edu.cn

including H (hierarchical) B-splines, T-splines, PHT- (polynomial) splines (over hierarchical T-meshes) and LR (locally refined) B-splines. We briefly review these splines, emphasizing PHT-splines and LR B-splines as these are particularly relevant for our paper:

- HB-splines were established by Forsey and Bartels [9] for applications in geometric design. The initial lack of linear independence was resolved in the PhD thesis of Kraft [19] and further investigated by Vuong et al. [27]. Unfortunately, the partition of unity property is not preserved by the construction mechanism. As a remedy, Giannelli et al. [11] modified the basis by introducing the truncation mechanism, which resulted in the definition of THB-splines. These combine good approximation and stability properties and have been shown to be useful for geometric design and IGA [10, 17].
- T-splines were invented by Sederberg et al. [25] as a surface design methodology. Later they were then used for IGA [1]. Buffa et al. studied their linear independence [4], indicating that this property is not guaranteed on generic T-meshes. Subsequently, Li et al. [20] introduced the restricted subset of “analysis-suitable” T-splines, which are linearly independent and form a partition of unity.
- PHT-splines [7], which are piecewise bicubic polynomials with C^1 -continuity over hierarchical T-meshes, inherit several good properties of B-splines. Higher degree PHT-splines and the dimension of the space spanned by them were investigated in the paper [6]. Compared to other constructions, the reduced smoothness s for degree $p = 2s + 1$ simplifies the mathematical theory. PHT-Splines have been used for various applications, such as isogeometric analysis [18], topology optimization [14], domain parameterization [5], and fracture mechanics [29]. Later, it was observed that the basis of PHT-splines reveals a decay phenomenon for certain types of refinement of T-meshes [16], which is not expected in applications. Subsequently, several modified versions of PHT-splines [16, 22, 30] were proposed to address this issue.
- LR B-splines were introduced by Dokken et al. [8] and provide another way to perform adaptive refinement of spline spaces. The basic idea of LR B-splines is to extend the global refinement of B-splines to insertion of local line segments in tensor meshes. Although LR B-splines possess almost all the properties of classical B-splines, they are not always linearly independent. A useful analysis was carried out by Bressan [2]. Subsequently, Bressan and Jüttler [3] presented a hierarchical construction of LR-spaces which guarantees the local linear independence of basis functions and completeness. In [23], the authors studied the necessary features of LR B-splines to have the linear independence property and proved that the minimal number of LR B-splines needed for this property is eight. Patrizi et al. [24] further proposed a practical refinement strategy that ensures the local linear independence of the resulting LR B-splines. Several applications of LR B-splines in isogeometric simulations and geometric modeling can be found in the literature [13, 15, 26].

Recently, we proposed [12] a simple algorithm which constructs hierarchical T-meshes by repeatedly inserting new line segments, focusing on the case of LR B-

splines for bilinear (i.e., C^0 -smooth) PHT-splines. The main benefit of this approach is the ability to adapt both the shape and size of the cells to the specific application, while ensuring the good properties of local linear independence and partition of unity of the basis. The correctness of this algorithm was verified by enumerating the newly introduced standardized local configurations.

Based on this work, which mainly focused on the bilinear case and on the concept of semi-regularity in the sense of Weller and Hagen [28], the present paper extends and improves the construction in several ways: First, the new algorithm is applicable to higher order splines of degree $p = 2s + 1$ with C^s -smoothness. Second, two new mesh quality parameters that measure the local complexity and quality of the elements are introduced. In order to make the paper self-contained, we also include a new proof of the fact (first noted by Dokken et al. [8]) that the resulting LR B-splines depend solely on the final mesh.

The remainder of the paper is organized as follows. The construction of locally linearly independent LR B-splines on PHT spline spaces is reviewed in Section 2. The next two sections introduce the RMB-spline systems and analyzes the B-splines systems on the cells with the help of standardized local configurations. The proposed refinement algorithm is established in Sections 5 and 6 with the help of the notion of good line segments. Numerous experimental results are shown in Section 7. The final section draws the conclusions and identifies directions for future work.

2 Preliminaries

Our starting points are the sets of *vertical* and *horizontal line segments*

$$v = \{x_v\} \times [y_v, y'_v] \quad \text{and} \quad h = [x_h, x'_h] \times \{y_h\},$$

respectively, where $x_v, y_v, y'_v, y_h, x_h, x'_h \in \mathbb{R}$ and $y_v < y'_v$ and $x_h < x'_h$. A *T-mesh* M covering the *domain* Ω (which will be introduced later) is represented by a finite set of line segments, which is saturated in the sense that we always use the longest possible segments for representing it¹. The subset relation is generalized to meshes by writing $M \sqsubset M'$ whenever each line segment in M is a subset of a line segment in M' .

The *cells* c of the mesh are the bounded connected components of the set difference $\Omega \setminus M$, where the symbol \setminus indicates that we apply the set difference operator with respect to all the elements of M . Furthermore, we exclude non-rectangular cells by assuming that the mesh can be created from an initial tensor mesh by iteratively inserting one vertical or horizontal line segment at a time, such that the two end points of that segment are located on segments that are already present at this step.

On each mesh we define collections of *systems of B-splines*. Each system β consists of $(s + 1)^2$ B-splines of degree $p = 2s + 1$ that are C^s smooth for $s \geq 1$,

¹ More precisely, all pairs of parallel line segments in M (i.e., both vertical or both horizontal) have no common point.

which are specified by the local knot vectors $X_\beta = [x, x', x'']$ and $Y_\beta = [y, y', y'']$ with $x < x' < x''$ and $y < y' < y''$ and possesses the associated mesh

$$G_\beta = \{ \{\xi\} \times [y, y''] : \xi \in \{x, x', x''\} \} \cup \{ [x, x''] \times \{\eta\} : \eta \in \{y, y', y''\} \},$$

which we call its *grid*. All these B-splines take the form

$$N_{\Xi}^p(x) N_{\mathbb{H}}^p(y),$$

where the local knot vectors Ξ and \mathbb{H} of the univariate B-splines consist of $p + 2$ instances of the knots x, x', x'' and y, y', y'' , respectively, with the multiplicities $k, s + 1$ and $s + 2 - k$ of the first, second and third knot, respectively, for $k = 1, \dots, s + 1$. As an example, Fig. 1 visualizes the knot vectors of the B-splines forming a system for $s = 1$. The axis-aligned box $[x, x''] \times [y, y'']$ is the *support* of the B-spline

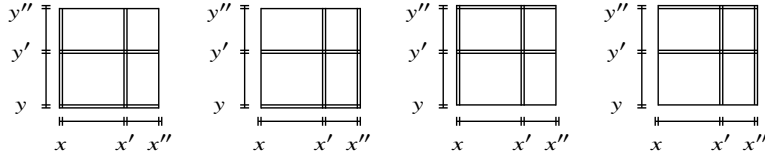


Fig. 1: A B-spline system for $s = 1$. It consists of four bicubic B-splines and the knot lines have multiplicity 1 or 2.

system, and (x', y') serves as its *anchor point*. A B-spline system is said to be *on the mesh* M if its grid satisfies $G_\beta \sqsubset M$, and the collection of the B-spline systems on the mesh forms the set B . Note that B depends on M ! Clearly, nested meshes possess nested collections of B-spline systems, $B' \subset B$ if $M' \sqsubset M$. Here we use the prime $'$ to denote a second mesh and the associated collection of the B-spline systems.

The following example will be used throughout the paper in order to illustrate the theory presented:

Example We consider meshes $M \sqsupset M_0$ that contain the initial mesh

$$M_0 = \{ \{x\} \times [a - 1, b + 1] : x \in \{a - 1, a, b, b + 1\} \} \cup \{ [a - 1, b + 1] \times \{y\} : y \in \{a - 1, a, b, b + 1\} \},$$

where we use the phantom knots $a - 1$ and $b + 1$. The 16 B-spline systems on the initial mesh M_0 form the set B_0 . \diamond

A B-spline system $\beta \in B$ is said to *split into* another B-spline system $\beta' \in B$ with respect to the mesh M , denoted by

$$\beta \rightarrow_M \beta' \quad \text{and} \quad \beta' = (\beta : \ell)_{+/-},$$

if the grids satisfy $G_{\beta'} \subset (G_\beta \sqcup \{\ell\})$ for some (vertical or horizontal) line segment $\ell \in M$. More precisely, ℓ is a subset of an element of M , and we use the symbol \sqsupseteq to denote this generalized element notation. The sign $+$ or $-$ indicates which of the two resulting systems is selected, see Fig. 2. Moreover, it is required that the line

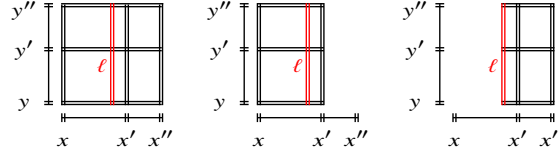


Fig. 2: The B-spline system β (left) splits into $(\beta:\ell)_-$ (middle) and $(\beta:\ell)_+$ (right).

segment ℓ traverses the support of β and is not already present in its grid, and the satisfaction of these conditions is indicated as $\ell \mid \beta$. In addition we define

$$(\beta:\ell)_{+/-} = \beta \quad \text{if} \quad \ell \nmid \beta.$$

The “splits into” relation \rightarrow_M defines the *directed acyclic graph* $\Gamma = (B, \rightarrow_M)$ with vertex set B . The sinks of this graph, which form the set B^+ , are the *minimally supported B-spline systems* on the mesh M .

3 The reachable minimally supported B-spline systems

We consider a subset $S \subseteq B$, which is called the set of *seeds*. Among all the B-spline systems on a given mesh M , we are only interested in those that can be generated by splitting one of the seed systems, and we denote the resulting subset of B by

$$\{S \rightarrow_M^+\} = \{\beta \in B : \exists \beta_0 \in S \text{ such that } \beta_0 \rightarrow_M^+ \beta\},$$

where \rightarrow_M^+ denotes the transitive closure of the relation \rightarrow_M . In particular, we will study the systems of *reachable minimally supported B-spline systems (RMB-spline systems)* on the mesh M ,

$$R = \{S \rightarrow_M^+\}^\perp = \{\beta \in \{S \rightarrow_M^+\} : \beta \text{ is a sink}\}. \quad (1)$$

Example We choose the four sinks in B_0 as the set of seeds S_0 . These four B-spline systems also form the RMB-spline systems on M_0 . \diamond

Consider a coarser mesh $M' \subset M$. We analyze the sinks that can be found by tracing a path in Γ that starts at one of the vertices in the set $R' = \{S \rightarrow_{M'}^+\}^\perp$ in order to establish the following theorem, which is a reformulation (with a new proof) of

Theorem 3.4 by Dokken et al. [8]. We include it here in order to make this article self-contained:

Theorem 1 *The RMB-spline systems on a mesh M can be reached from the RMB-spline systems on any coarser mesh $M' \sqsubset M$, i.e.,*

$$\{R' \rightarrow_M^+\}^\perp = R,$$

provided that both M and M' are derived from the same set of seeds $S = S' \subset B' \subset B$, where B and B' are the collections of the B-spline systems on the meshes M and M' , respectively.

Proof We prove the theorem by contradiction. Assume there exists a RMB-spline system $\beta_\perp \in R$ that cannot be reached from a RMB-spline system in R' . We consider all the paths of B-spline systems that start at an element $\beta_0 \in S$ and terminate at $\beta_\perp \in R$. Let $\hat{\beta}^{(0)}$ be the first B-spline system on some path whose successor $\hat{\beta}^{(1)}$ is not on the coarse mesh M' , i.e., $\hat{\beta}^{(1)} \notin B'$. Among all the paths and B-spline systems $\hat{\beta}$ we pick the ones where the area of the support is minimal. By assumption, $\hat{\beta}^{(0)}$ is not a sink with respect to $\rightarrow_{M'}$, hence there exists a line segment $k \in M'$ such that the two systems $(\hat{\beta} : k)_{+/-}$ are on M' . The remaining path $\hat{\beta}^{(0)}, \hat{\beta}^{(1)}, \hat{\beta}^{(2)}, \dots, \hat{\beta}^{(n)} = \beta_\perp$ with associated line segments $\ell^{(i)}$ used in the splitting steps,

$$\hat{\beta}^{(i+1)} = (\hat{\beta}^{(i)} : \ell^{(i)})_{+/-} \quad (2)$$

will be called the *tail*. We will show that there exists a modified tail $\bar{\beta}^{(0)}, \bar{\beta}^{(1)}, \bar{\beta}^{(2)}, \dots, \bar{\beta}^{(n)} = \beta_\perp$ such that its vertices satisfy the two conditions

$$\bar{\beta}^{(i)} = (\hat{\beta}^{(i)} : k)_{+/-} \quad (3a) \quad \text{and} \quad \bar{\beta}^{(i+1)} = (\bar{\beta}^{(i)} : \ell^{(i)})_{+/-} \quad (3b)$$

for a suitable choice of the signs. Some of the adjacent nodes may be identical (if $\ell^{(i)} \uparrow \bar{\beta}^{(i)}$) and can be merged.

In order to prove the existence of the modified tail, we note that the splitting steps with respect to $\ell^{(i)}$ and k commute in the sense that two sets

$$\{((\hat{\beta}^{(i)} : k)_+ : \ell^{(i)})_+, ((\hat{\beta}^{(i)} : k)_+ : \ell^{(i)})_-, ((\hat{\beta}^{(i)} : k)_- : \ell^{(i)})_+, ((\hat{\beta}^{(i)} : k)_- : \ell^{(i)})_-\} \text{ and} \\ \{((\hat{\beta}^{(i)} : \ell^{(i)})_+ : k)_+, ((\hat{\beta}^{(i)} : \ell^{(i)})_+ : k)_-, ((\hat{\beta}^{(i)} : \ell^{(i)})_- : k)_+, ((\hat{\beta}^{(i)} : \ell^{(i)})_- : k)_-\}$$

are identical since both sets consist of the minimally supported B-spline systems on the mesh obtained by adding k and $\ell^{(i)}$ to $G_{\beta^{(i)}}$, which is a tensor mesh when restricted to the support of $\beta^{(i)}$, see Fig. 3. The figure depicts one representative for each class of topologically equivalent configurations. Additional (simpler) cases arise if k is identical to one of the other line segments.

Hence, we may construct the modified tail going backward from the sink β_\perp to $\hat{\beta}^{(0)}$ by choosing the sign in the first equation in (3) such that the second condition is satisfied for $i = n - 1, \dots, 0$. Indeed, considering the diagram in Fig. 4, for any given $\hat{\beta}^{(i)}, \hat{\beta}^{(i+1)}$ and $\bar{\beta}^{(i+1)}$ that respect the upper and the right arrow, the equality

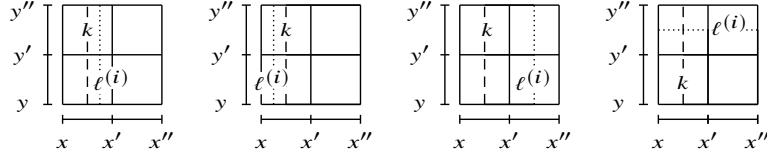


Fig. 3: The mesh $G_{\beta^{(i)}} \sqcup \{k\} \sqcup \{\ell^{(i)}\}$ is a tensor mesh in all the situations.

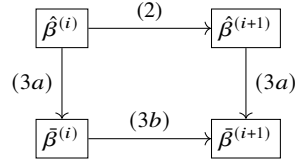


Fig. 4: The commutativity of this diagram ensures the existence of the modified tail.

of the two sets implies that one may always find a $\bar{\beta}^{(i)}$ ensuring commutativity for some choice of signs of the splitting steps on the lower and the left arrow.

Summing up, we obtain a new path that starts at $\beta_0 \in S$ and terminates at $\beta_\perp \in R$, simply by replacing the tail with the modified tail. Again, we consider the first B-spline system on the path whose successor is not on the coarse mesh M' . This system is necessarily behind $\hat{\beta}$, since $\bar{\beta}^{(0)}$ is on the coarse mesh \hat{M} . Consequently, the area of its support is smaller than the support area of $\hat{\beta}$, in contradiction to the assumption regarding the minimal support area. \square

This theorem leads to a procedure for generating the RMB-spline systems on a mesh: One inserts one line segment after the other. After each insertion, splitting steps are used to transform the RMB-spline systems of the previous instance of the mesh to the current one. Clearly, one needs to consider all the line segments that are present in the mesh at this stage, since the latest line segment insertion may enable additional splitting steps with respect to previously inserted ones.

4 The B-spline systems on the cells

The B-spline system $\beta \in B$ is said to be *active on the cell* c if $c \subset \text{supp}(\beta)$. The *active RMB-spline systems* on a cell c form the set

$$R_c = \{\beta \in R : c \subseteq \text{supp} \beta\}.$$

Furthermore, the *local mesh*

$$M_c = \bigsqcup_{\beta \in R_c} G_\beta$$

of a cell is the union of all the local grids G_β associated with B-spline systems $\beta \in R_c$.

We introduce the notion of *standardized local configurations* (SLCs) in order to capture the topologically different collections of active RMB-spline systems on the cells. An SLC is a finite collection of B-spline systems

$$\Sigma = \{\beta_1, \beta_2, \dots, \beta_{n_\Sigma}\}$$

where all the knots are odd integers, such that all the supports contain the standard cell $[-1, 1]^2$. Moreover, it is required that the cell's knot vectors (i.e., the union of the knot vectors, which are considered as sets for notational convenience) combined with the cell's boundary knots, i.e.,

$$\bigcup_{i=1}^{n_\Sigma} X_{\beta_i} \cup \{-1, +1\} \quad \text{and} \quad \bigcup_{i=1}^{n_\Sigma} Y_{\beta_i} \cup \{-1, +1\}$$

are finite sequences of *consecutive* odd integers. Note that we consider SLCs as equivalent if there exist reflections or rotations that transform them into each other.

For each cell c there exists a homeomorphism h_c of the plane \mathbb{R}^2 that transforms c into $[-1, 1]^2$ and R_c into an SLC

$$\Sigma_c = \{\beta : \exists \beta' \in R_c \text{ such that } G_\beta = h_c(G_{\beta'})\}.$$

The resulting SLC is unique up to reflections and rotations, and thus we will denote it as *the standardized local configuration of the cell c* .

We consider two meshes M and M' with cells c and c' and associated SLCs $\Phi = \Sigma_c$ and $\Phi' = \Sigma_{c'}$, respectively. The SLC Φ is said to *refine into* the SLC Φ' , denoted by $\Phi \rightsquigarrow \Phi'$, if

- (i) $c' \subseteq c$,
- (ii) $R_c \neq R_{c'}$ and
- (iii) there exists a line segment k such that $M \sqcup \{k\} = M'$.

The second condition is imposed in order to exclude the insertion of line segments that do not enrich the spline space (e.g., segments that split a single cell only).

Among all the SLCs we consider the finite subset \mathcal{F} of all the standardized configurations with only *four* elements,

$$\mathcal{F} = \{\Sigma : \Sigma \text{ is SLC and } |\Sigma| = n_\Sigma = 4\},$$

since this is a necessary condition for the associated spline spaces to possess the property of local linear independence. Among others it contains the *tensor-product standardized local configuration* T , which is depicted in Fig. 5 (left). The figure shows the mesh (solid black lines), the standard cell (blue) and the anchor points (x', y') of the B-spline systems (red squares).

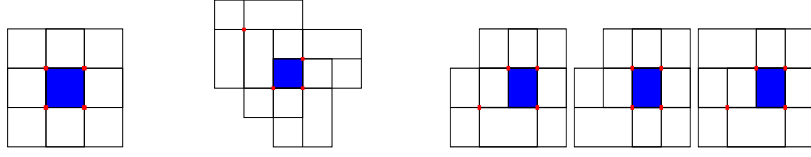


Fig. 5: Left: $\mathcal{E}_{4,4} = \{T\}$. Center: An SLC in $\mathcal{F} \setminus \{T \rightsquigarrow_{\mathcal{F}}^+\}$. Right: $\mathcal{E}_{4,5}$.

We denote with $\rightsquigarrow_{\mathcal{F}}$ the restriction of the “refines into” relation to \mathcal{F} ,

$$\Phi \rightsquigarrow_{\mathcal{F}} \Phi' \quad \text{if} \quad \Phi \rightsquigarrow \Phi' \quad \text{and} \quad \Phi, \Phi' \in \mathcal{F}.$$

The symbol $\rightsquigarrow_{\mathcal{F}}^+$ denotes the transitive closure of this relation. Similar to \rightarrow_M , it defines a directed acyclic graph $(\mathcal{F}, \rightsquigarrow_{\mathcal{F}})$.

We recall the following result about the SLCs that are created by refining the tensor-product configuration:

Lemma 1 *The set of SLCs*

$$\{T \rightsquigarrow_{\mathcal{F}}^+\} = \{\Phi \in \mathcal{F} : T \rightsquigarrow_{\mathcal{F}}^+ \Phi\}$$

that are reachable from the tensor-product SLC T via $\rightsquigarrow_{\mathcal{F}}$ consists of the 385 elements (up to reflections and rotations) listed in the Appendix of [12, technical report version].

Proof All the SLCs Φ' a given configuration Φ refines into can be generated by taking the mesh and the seeds

$$M = \bigsqcup_{\beta \in \Phi} G_{\beta} \quad \text{and} \quad S = \Phi,$$

respectively, and then considering all the meshes M' that are obtained by adding a single line segment k to it. It suffices to analyze one representative from each class of line segments that lead to topologically equivalent meshes. Hence we can reduce the problem to a finite number of cases for each SLC. Based on this fact, the result was obtained in [12] by recursively enumerating the reachable standardized local configurations, starting with T . \square

Note that $\{T \rightsquigarrow_{\mathcal{F}}^+\}$ is a proper subset of \mathcal{F} . To confirm this fact, Fig. 5 (center) shows an instance of an SLC (i.e., the mesh and the anchor points) that belongs to \mathcal{F} but not to $\{T \rightsquigarrow_{\mathcal{F}}^+\}$.

We are interested in several subsets of $\{T \rightsquigarrow_{\mathcal{F}}^+\}$: Firstly, we introduce the sets $\mathcal{E}_{q,r}$, where $4 \leq q \leq r$, that contain all the SLCs in $\{T \rightsquigarrow_{\mathcal{F}}^+\}$ with *exactly* q and r knots, respectively, in one direction and in the other direction. Table 1(left) lists the number of SLCs in these sets up to reflections and rotations. Figs. 5–15 visualize selected SLCs (meshes and anchor points) in these sets.

q	r						τ	μ				
	4	5	6	7	8	≥ 9		4	5	6	7	≥ 8
4	1	3	15	18	12	0	8	1	1	1	1	1
5	n/a	11	56	72	36	0	9	1	4	4	4	4
6	n/a	n/a	50	72	39	0	10	1	15	30	30	30
≥ 7	n/a	n/a	n/a	0	0	n/a or 0	11	1	15	86	104	104
							12	1	15	136	226	238
							13	1	15	136	298	346
							≥ 14	1	15	136	298	385

Table 1: Number of SLCs in $\mathcal{E}_{q,r}$ (left) and in $\mathcal{K}_{\mu,\tau}$ (right).

Secondly, we establish the sets $\mathcal{K}_{\mu,\tau}$ of SLCs with at most τ knots that have no more than μ knots in each direction. The indices μ and τ are called the *maximum* and the *total knot number*, respectively. These sets satisfy

$$\mathcal{K}_{\mu,\tau} = \bigcup_{q \leq r \leq \mu, q+r \leq \tau} \mathcal{E}_{q,r}.$$

Table 1(right) reports the numbers of SLCs in these sets up to reflections and rotations.

5 Good line segments

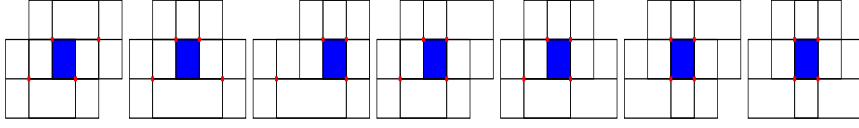
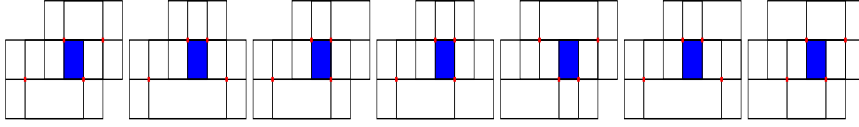
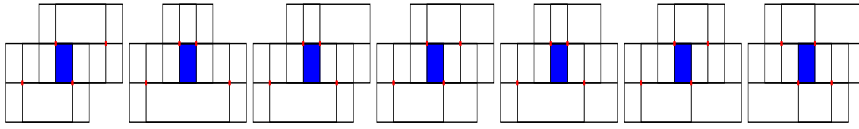
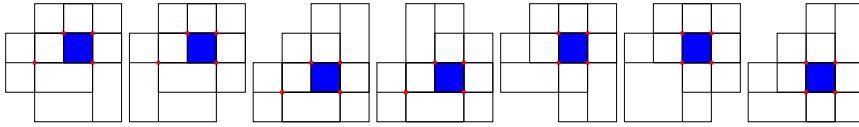
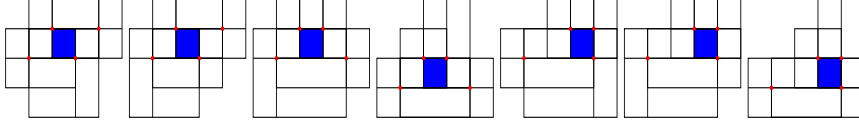
Consider a fixed set of seeds S and a domain $\Omega \subset \mathbb{R}^2$. A mesh M is said to be (S, Ω) -compatible if

- (i) the B-spline systems in S are on the mesh M and
- (ii) the domain Ω is equal to the closure of the union of a subset of the cells of the mesh M .

The cells contained in the latter subset (and hence in the domain) are said to be *active*.

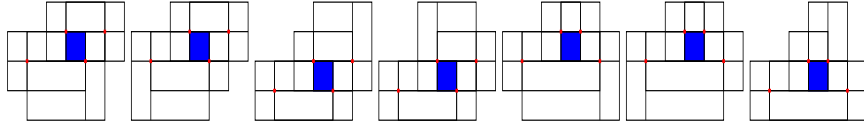
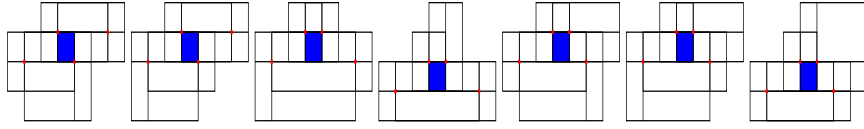
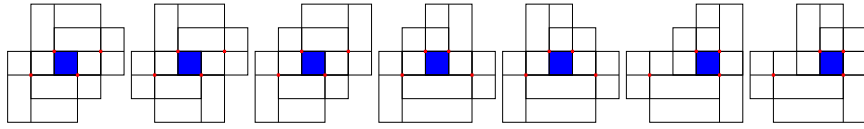
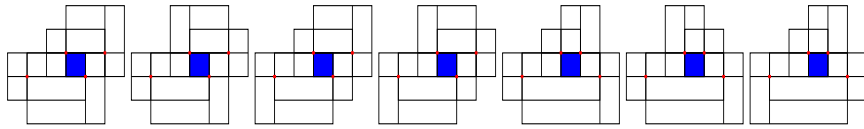
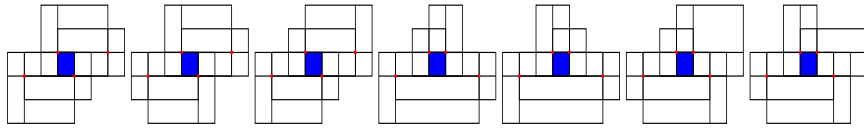
Based on the sets $\mathcal{K}_{\mu,\tau}$ of SLCs, we introduce the following notion: A compatible mesh M – with the associated RMB-splines R obtained from S – is said to have the *class* (μ, τ) if all the SLCs of all active cells belong to $\mathcal{K}_{\mu,\tau}$. The quantities μ and τ are called the *mesh quality parameters*. Clearly, a mesh has such a class only if all the SLCs belong to $\{\mathbb{T} \rightsquigarrow_{\mathcal{F}}^+\} = \mathcal{K}_{8,14}$. The class (∞, ∞) is assigned otherwise. In particular, this class is assigned to meshes with cells that possess more than four active systems of B-splines and to meshes containing line segments that do not enrich the spline space, according to the second condition (ii) in the definition of the “refines into” relation for SLCs.

The class of a mesh will be used to control the *local complexity* of the elements. The larger the mesh quality parameters, the richer the set of SLCs that may be present in the mesh.

Fig. 6: Selected SLCs in $\mathcal{E}_{4,6}$.Fig. 7: Selected SLCs in $\mathcal{E}_{4,7}$.Fig. 8: Selected SLCs in $\mathcal{E}_{4,8}$.Fig. 9: Selected SLCs in $\mathcal{E}_{5,5}$.Fig. 10: Selected SLCs in $\mathcal{E}_{5,6}$.

A vertical or horizontal line segment ℓ is said to be *good for the class* (μ, τ) if the class of the mesh $M \sqcup \{\ell\}$ – with the associated RMB-splines on it – does not exceed (μ, τ) . Furthermore, we specialize this notion to the local mesh M_c , which was introduced for all the cells c of M . Here we use the RMB-splines R_c on the cell as the set of seeds and the cell itself as the domain, hence we consider M_c as a (R_c, c) -compatible mesh and assume it has class (μ, τ) . This is the case if the SLC belongs to $\mathcal{K}_{\mu, \tau}$. We then say that a line segment ℓ is *locally good for the class* (μ, τ) with respect to the cell c if the class of the mesh $M_c \sqcup \{\ell\}$ – which is again (R_c, c) -compatible – does not exceed (μ, τ) .

Local goodness implies global goodness: A line segment ℓ is good for the class (μ, τ) if and only if it is locally good for this class with respect to all the cells. The following result provides a *sufficient* condition for local goodness:

Fig. 11: Selected SLCs in $\mathcal{E}_{5,7}$.Fig. 12: Selected SLCs in $\mathcal{E}_{5,8}$.Fig. 13: Selected SLCs in $\mathcal{E}_{6,6}$.Fig. 14: Selected SLCs in $\mathcal{E}_{6,7}$.Fig. 15: Selected SLCs in $\mathcal{E}_{6,8}$.

Lemma 2 *Line segments that traverse a local mesh M_c of some class (μ, τ) are always² locally good with respect to the cell c .*

Proof We go through all the 385 SLCs in $\{\mathcal{T} \rightsquigarrow_{\mathcal{F}}^+\}$ and add all the possible line segments ℓ that traverse the local meshes M_c with $c = [-1, 1]^2$. It suffices to analyze one representative for each class of topologically equivalent meshes $M_c \sqcup \{\ell\}$, hence we arrive at a finite number of cases. A detailed analysis confirms the above result.

More precisely, for each SLC we generate all the vertical lines $x = \xi$ and all the horizontal lines $y = \eta$ with integer coordinates $\xi, \eta \in \mathbb{Z}$. We consider only the lines among them that intersect the local mesh M_c in a non-empty line segment ℓ . The number of these lines and associated line segments is finite.

² i.e., for all values of the mesh quality parameters μ and τ

Finally, we compute the class of $M_c \sqcup \{\ell\}$ for each line segment ℓ and compare it with the class of M_c . It turns out that the class never increases. More precisely, we obtain the same or a lower class for all the 385 SLCs and for all the considered lines and associated line segments. \square

The lemma forms the basis for a procedure that turns any line segment ℓ into a good line segment, simply by extending it as long as this is necessary. It confirms that the two mesh quality parameters μ and τ are compatible with this procedure, which is formalized as Algorithm GOODLINESEGMENT.

Algorithm: GOODLINESEGMENT(line segment ℓ)

```

global mesh  $M$ ; class  $(\mu, \tau)$ ;
LineSegmentGrows  $\leftarrow$  true;
while LineSegmentGrows do
    LineSegmentGrows  $\leftarrow$  false;
     $M' \leftarrow M \sqcup \{\ell\}$ ;
    forall cells  $c'$  of mesh  $M'$  do
        if  $\Sigma_{c'} \notin \mathcal{K}_{(\mu, \tau)}$  then
            LineSegmentGrows  $\leftarrow$  true;
            forall cells  $c$  of mesh  $M$  do
                if  $c' \subseteq c$  then
                    extend  $\ell$  such that it traverses  $\bigcup_{\beta \in R_c} \text{supp } \beta$ ;
    return  $\ell$ ;

```

The algorithm uses the mesh M and its class (μ, τ) as global variables. In particular, the line segment will be extended if its insertion (or the insertion of some parts of it) do not enrich the spline space, according to the second condition (ii) in the definition of the “refines into” relation for SLCs.

6 Mesh refinement

Given a pair (μ, τ) of finite mesh quality parameters, we study the RMB-spline systems on sequences of meshes that are created via mesh refinement,

$$M^{(i)} = M^{(i-1)} \sqcup \{\ell^{(i-1)}\} \quad \text{and} \quad R^{(i)} = \{R^{(i-1)} \rightarrow_{M^{(i)}}^+\}^\perp \quad \text{for } i = 1, 2, \dots, N,$$

where we assume that a *good* vertical or horizontal line segment $\ell^{(i-1)}$ is inserted in each step. In addition, it is required that *the end points of that segment are located on segments that are already present* in the mesh at this step. The sequence starts with an initial mesh M^0 with RMB-spline systems $R^0 = \{S \rightarrow_{M^0}^+\}^\perp$ for a given set of seeds S .

The construction is justified by Theorem 1, which ensures that the iteratively created sets $R^{(i)}$ are indeed the RMB-spline systems $\{S \rightarrow_{M^{(i)}}^+\}^\perp$ on the mesh $M^{(i)}$, cf. (1). The goodness of the inserted line segments ensures that the class (μ, τ) of

the initial mesh³ is preserved throughout the refinement process. Consequently, the mesh quality parameters μ and τ are compatible with our construction.

We restrict the initialization of the refinement procedure in order to derive additional results, cf. Fig. 16.

Assumption The initial mesh $M^{(0)}$, the set of seeds S and the domain Ω fulfill the following three conditions:

- (i) The initial mesh $M^{(0)}$ is a tensor mesh.
 - (ii) The seeds S are all the associated tensor-product B-splines with knots possessing multiplicity $s + 1$, organized in systems associated with the inner vertices of the initial mesh.
 - (iii) The domain Ω is the closure of the union of a certain subset of the cells (including the cell's boundaries) that does not contain any of the boundary cells of $M^{(0)}$. Its boundary consists of closed simple curves, which are mutually disjoint.
- ◇

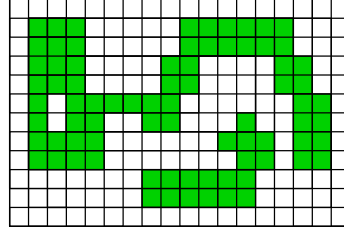


Fig. 16: An initial mesh (black) and a domain (green) that fulfills the assumption.

Example We choose the initial mesh $M^{(0)} = M_0$, the seeds $S = S_0$ and the domain $\Omega = [a, b]^2$. The assumption is satisfied. ◇

The spaces spanned by the RMB-spline systems $R^{(i)}$ are nested,

$$\text{span} \bigcup_{\beta \in R^{(i-1)}} \beta \subseteq \text{span} \bigcup_{\beta \in R^{(i)}} \beta,$$

simply because any B-spline in β admits a representation as a linear combination (with non-negative weights) of the functions in $(\beta:\ell)_+ \cup (\beta:\ell)_-$ for any line segment ℓ . These spaces also contain all the tensor-product polynomials of degree (p, p) restricted to Ω , since the domain does not contain the boundary cells of the initial tensor mesh.

Theorem 2 The RMB-spline systems $R^{(i)}$

³ That mesh even possesses the class $(8, 4)$, due to the assumption, as all the SLCs are equal to T.

- (i) are locally linearly independent on the domain Ω , and
- (ii) form a nonnegative partition of unity on Ω .

In addition, they

- (iii) span the full spline space defined by Ω and $M^{(i)}$

if the mesh contains no T -vertices⁴ on the domain boundary.

Proof All the SLCs of the created meshes possess the class (μ, τ) , thus the unions of the RMB-spline systems $R_c^{(i)}$ on each cell c of $M^{(i)}$ are linearly independent since $|R_c^{(i)}| = 4$ and the space spanned by them contains all the tensor-product polynomials of degree (p, p) restricted to c . Indeed, these polynomials form a linear space of dimension $(p+1)^2 = (2s+2)^2 = 4(s+1)^2$ and this number is equal to the total number of B-splines in the four systems in $R_c^{(i)}$. The linear independence of the unions of the RMB-spline systems $R_c^{(i)}$ on c implies the local linear independence (i).

The proof of the second statement relies on two facts:

- Firstly, the anchor points of the active⁵ B-spline systems belong to Ω . This is true for the initial mesh and for the RMB-splines on it (which are simply the seeds). It carries over to the subsequent meshes since this property is preserved by the splitting steps. (Note that the lines spanned by the segments of the domain boundary traverse the entire domain Ω as they belong to the initial tensor mesh $M^{(0)}$.)
- Secondly, no anchor point of any active B-spline system is contained within the interior of the support of any other B-spline system. This fact is verified with the help of a detailed analysis of the SLCs in $\{T \rightsquigarrow_{\mathcal{F}}^+\}$.

Since the space spanned by the RMB-splines $R^{(i)}$ contains the tensor-product polynomials of degree (p, p) on the domain Ω , we may recover the representation of the function $f(x, y) = 1$ by interpolating its values and derivatives. In particular, we interpolate the value $f(x, y) = 1$ and the partial derivatives $\partial_x^j \partial_y^k f(x, y) = 0$ for $j, k = 0, \dots, s$, $(j, k) \neq (0, 0)$, at all the anchor points of the active B-spline systems, based on the first fact. The number of these anchor points is equal to the number of systems and they are all contained within Ω . The second fact ensures that the resulting linear equations splits into $|R^{(i)}|$ sets of equations that can be solved individually, one for each active B-spline system and its anchor point. Solving them individually confirms that choosing all the B-spline coefficients equal to 1 gives a partition of unity. This proves the second statement (ii) since all the B-splines are non-negative.

The full spline space defined by Ω and $M^{(i)}$ has been analyzed in [6], where it was shown that its dimension is equal to $(C + B)(s + 1)^2$, where C is the number of the domain's inner cross vertices and B is the number of the boundary vertices. There are $(C + B)$ active RMB-spline systems on Ω since the mesh contains no T -vertices

⁴ This can be guaranteed easily by extending all the line segments that reach the domain boundary such that they traverse one more cell of the mesh.

⁵ i.e., the ones that take non-zero values on the domain Ω

on the domain boundary. This completes the proof, since the active RMB-splines are linearly independent on Ω and each system consists of $(s + 1)^2$ tensor-product B-splines. \square

7 Experiments

We verify the effectiveness of the new algorithm by performing the adaptive approximation of three functions over the square $[1, 11]^2$. Starting from a domain covered by a tensor mesh which contains 10×10 cells with 121 systems of basis functions, the adaptive approximation procedure runs until the given precision (with respect to the maximum error) is achieved, see [12, Section 6] for a more detailed description. All the examples were run in C++ using the open-source library G+smo [21] developed for isogeometric analysis. For simplicity we use $s = 0$ and $p = 1$ since the mesh refinement can be guided efficiently in this situation.

More precisely, the refinement procedure is guided by a marking procedure (identifying the cells that need to be refined based on the error) and a direction indicator (specifying the preferred direction of the split). While our direction indicator works well in the bilinear case, additional work is needed in order to extend it to higher degrees. This is beyond the scope of the present paper.

Instead, we focus on studying the effect of the class parameters μ and τ on the resulting meshes. In addition we will introduce the *element shape constraint* (ESC) in order to control the *quality* of the elements. In order to avoid non-aligned T-joints, we always use dyadic splits during the refinement process, as introduced in [12, Section 6.2].

7.1 Influence of the class parameters μ and τ

First we perform the adaptive refinement of the three peak function

$$f(x, y) = \sum_{k=1}^3 \exp\left(-10\sqrt{(x-3k)^2 + (y-3k)^2}\right) \quad (4)$$

using several values of μ . In this example, the parameter τ is set as ∞ and the tolerance ϵ is chosen to be 0.04 and 0.02, respectively.

Figure 17 presents the resulting meshes with different values of μ varying from 5 to 8. Here we only show the meshes for $\epsilon = 0.04$ since the lines of the ones for $\epsilon = 0.02$ are too detailed for a visualization, and this will be similar in the next examples. The figure indicates that choosing a smaller value of μ results in excess refinements, which is also verified by the number of basis functions listed in Table 2.

Second we consider approximations of the circular arc function

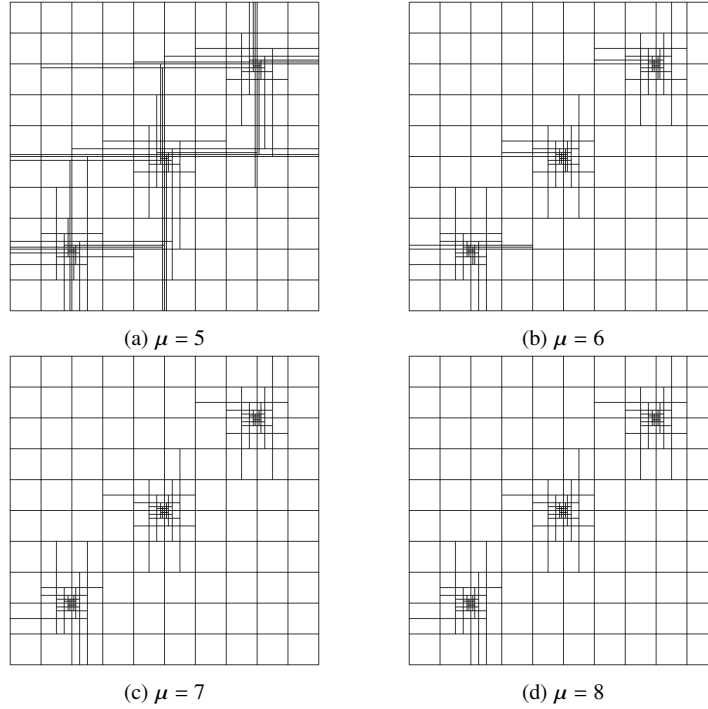


Fig. 17: The resulting meshes of approximating the three peak function (4) adaptively for different values of μ . The class parameter τ is set as ∞ in this example.

$$f(x, y) = 0.0615|(x - 1.5)^2 + (y - 1)^2 - 9.5^2| \quad (5)$$

for various values of τ . In this example, the class parameter μ is set as ∞ and the tolerance ϵ is chosen to be 0.04 and 0.02, respectively.

Figure 18 shows the meshes obtained by approximating this function adaptively with various values of τ ranging from 9 to 12. Here we only show the meshes for $\epsilon = 0.04$. It demonstrates that larger values of τ improve the mesh quality. The number of basis functions shown in Table 3 also supports this.

7.2 Adaptive refinement with element shape constraint

It is observed in Figure 17 and 18 that the shape of some cells is extremely uneven. More precisely, the ratio of width to height (height to width) of these cells is quite large. To this end, we further modify the framework of the original adaptive approximation algorithm by introducing the element shape constraint. Given the

Functions / Meshes	μ	$\epsilon = 0.04$	$\epsilon = 0.02$
Three peak function (4) Figure 17	5	409 (152%)	861 (148%)
	6	281 (104%)	621 (107%)
	7	269 (100%)	580 (100%)
	8	269 (100%)	580 (100%)
Circular arc function (5)	5	1,316 (163%)	2,774 (160%)
	6	887 (110%)	1,922 (112%)
	7	812 (101%)	1,742 (101%)
	8	805 (100%)	1,719 (100%)
Diagonal function (6)	5	1,999 (157%)	4,439 (177%)
	6	1,402 (110%)	2,705 (108%)
	7	1,307 (103%)	2,532 (101%)
	8	1,271 (100%)	2,509 (100%)

Table 2: The influence of the class parameter μ on the number of basis functions. Here the parameter τ is set as ∞ and the ESC condition is switched off.

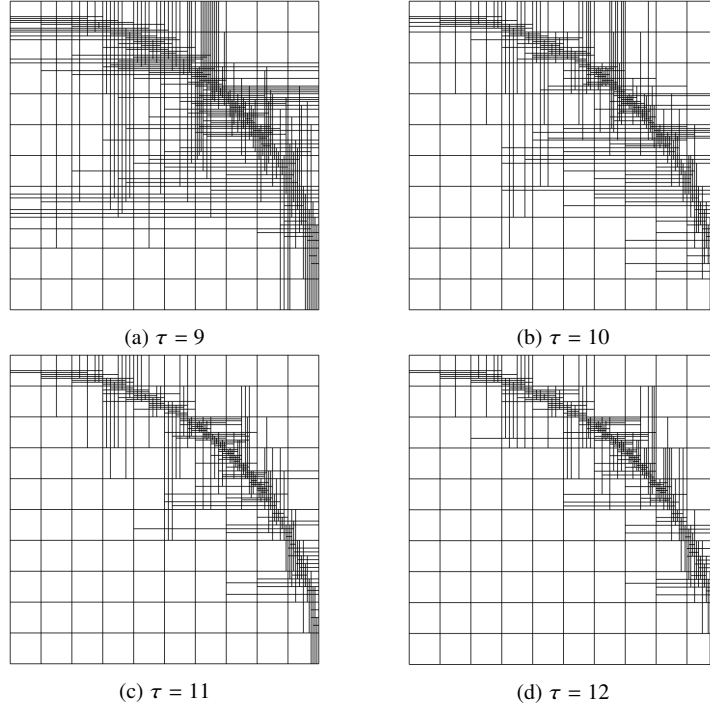


Fig. 18: The resulting meshes of approximating the circular arc function (5) adaptively using different values of τ . The class parameter μ is set as ∞ in this example.

Functions / Meshes	τ	$\epsilon = 0.04$	$\epsilon = 0.02$
Three peak function (4)	9	507 (188%)	1,131 (195%)
	10	296 (110%)	646 (111%)
	11	269 (100%)	585 (101%)
	12	269 (100%)	580 (100%)
Circular arc function (5) Figure 18	9	1,999 (242%)	4,533 (255%)
	10	1,178 (143%)	2,555 (144%)
	11	881 (107%)	1,913 (108%)
	12	825 (100%)	1,775 (100%)
Diagonal function (6)	9	3,558 (276%)	7,780 (301%)
	10	1,857 (144%)	4,122 (159%)
	11	1,457 (113%)	2,974 (115%)
	12	1,291 (100%)	2,586 (100%)

Table 3: The effect of the class parameter τ on the number of basis functions. Here the parameter μ is set as ∞ and the ESC condition is switched off.

upper bound for the ratio, denoted by ρ , the modified framework repeats the following steps:

1. Mark the cell with the largest shape ratio. If it is less than ρ , then continue with Step 4.
2. Extend the support of the marked cell and construct the corresponding split.
3. Perform the original refinement algorithm with the constructed split and continue with Step 1.
4. Mark the cell with the largest approximation error. If this error is less than ϵ , then exit.
5. Extend the support of the marked cell and construct the corresponding split.
6. Perform the original refinement algorithm with the constructed split and continue with Step 1.

We approximate the function

$$f(x, y) = |x - y| \quad (6)$$

adaptively using the modified algorithm. This function is non-smooth along the line $x - y = 0$. In this test, the class parameters μ and τ are both set as ∞ , the tolerance ϵ is also chosen to be 0.04 and 0.02, respectively.

Figure 19 depicts the resulting meshes with various values of ρ varying from 2 to 8. The one ($\rho = \infty$) obtained via the original approximation algorithm is also presented. Again only the meshes for $\epsilon = 0.04$ are shown. It reveals that smaller values of ρ lead to cells with better shapes, at the price of creating more basis functions as shown in Table 4.

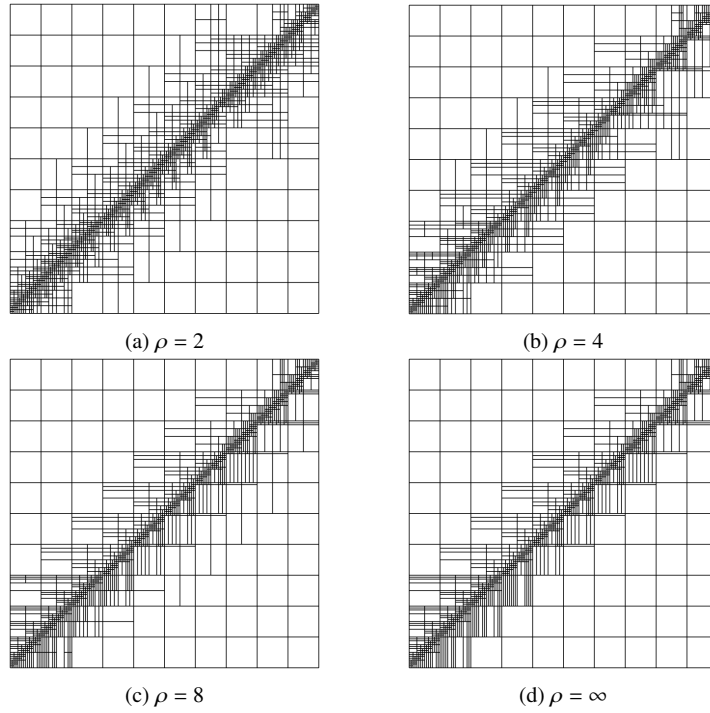


Fig. 19: The resulting meshes of approximating the diagonal function (6) adaptively using various ESC conditions. The class parameters μ and τ are both set as ∞ in this example.

8 Conclusion

The present paper extended the previous work [12], which mainly focuses on bilinear case, to C^s -smooth splines of degree $p = 2s + 1$. It introduced several new mesh quality parameters that measure the local complexity and quality of the elements. In addition, a new proof of the fact that the resulting B-splines depend solely on the final mesh was proposed in order to make the paper self-contained.

The current approach is only applicable to (PHT-) splines of degree $p = 2s + 1$ with C^s smoothness. Future work will address the extension to splines with more general combinations of smoothness s and degree $p > s$. Moreover, it is also worthwhile to explore the generalization to higher-dimensional splines. Last, but not least, the investigation of efficient data structures for this class of splines is also of vital interest.

Functions / Meshes	ρ	$\epsilon = 0.04$	$\epsilon = 0.02$
Three peak function (4)	2	271 (101%)	793 (137%)
	4	269 (100%)	582 (100%)
	8	269 (100%)	580 (100%)
	∞	269 (100%)	580 (100%)
Circular arc function (5)	2	1,249 (155%)	2,966 (173%)
	4	933 (116%)	2,001 (116%)
	8	821 (102%)	1,788 (104%)
	∞	805 (100%)	1,719 (100%)
Diagonal function (6) Figure 19	2	1,871 (147%)	3,900 (155%)
	4	1,495 (121%)	3,194 (127%)
	8	1,314 (109%)	2,681 (107%)
	∞	1,271 (100%)	2,509 (100%)

Table 4: The influence of the ESC condition on the number of basis functions. Here the class parameters μ and τ are both set as ∞ .

References

1. Y. Bazilevs, V. M. Calo, J. A. Cottrell, J. A. Evans, T. J. R. Hughes, S. Lipton, M. A. Scott, and T. W. Sederberg. Isogeometric analysis using T-splines. *Comput. Meth. Appl. Mech. Eng.*, 199(5-8):229–263, 2010.
2. A. Bressan. Some properties of LR-splines. *Comput. Aided Geom. Des.*, 30(8):778–794, 2013.
3. A. Bressan and B. Jüttler. A hierarchical construction of LR meshes in 2D. *Comput. Aided Geom. Des.*, 37:9–24, 2015.
4. A. Buffa, D. Cho, and G. Sangalli. Linear independence of the T-spline blending functions associated with some particular T-meshes. *Computer Methods in Applied Mechanics and Engineering*, 199(23-24):1437–1445, 2010.
5. C. L. Chan, C. Anitescu, and T. Rabczuk. Volumetric parametrization from a level set boundary representation with PHT-splines. *Computer-Aided Design*, 82:29–41, 2017.
6. J. Deng, F. Chen, and Y. Feng. Dimensions of spline spaces over T-meshes. *J. Comput. Appl. Math.*, 194(2):267–283, 2006.
7. J. Deng, F. Chen, X. Li, C. Hu, W. Tong, Z. Yang, and Y. Feng. Polynomial splines over hierarchical T-meshes. *Graphical Models*, 70(4):76–86, 2008.
8. T. Dokken, T. Lyche, and K. F. Pettersen. Polynomial splines over locally refined box-partitions. *Comput. Aided Geom. Des.*, 30(3):331–356, 2013.
9. D. R. Forsey and R. H. Bartels. Hierarchical B-spline refinement. In *Proceedings of the 15th annual conference on Computer Graphics and Interactive Techniques*, pages 205–212, 1988.
10. C. Giannelli, B. Jüttler, S. K. Kleiss, A. Mantzaflaris, B. Simeon, and J. Špeh. THB-splines: An effective mathematical technology for adaptive refinement in geometric design and isogeometric analysis. *Comput. Meth. Appl. Mech. Eng.*, 299:337–365, 2016.
11. C. Giannelli, B. Jüttler, and H. Speleers. THB-splines: The truncated basis for hierarchical splines. *Comput. Aided Geom. Des.*, 29(7):485–498, 2012.
12. L. Groiss, B. Jüttler, and M. Pan. Local linear independence of bilinear (and higher degree) B-splines on hierarchical T-meshes. *Comput. Aided Geom. Design*, 2023. to appear; available (including the appendix) as Technical Report no. 97 at www.ag.jku.at.
13. J. Gu, T. Yu, T.-T. Nguyen, Y. Yang, T. Q. Bui, et al. Fracture modeling with the adaptive XIGA based on locally refined B-splines. *Comput. Meth. Appl. Mech. Eng.*, 354:527–567, 2019.

14. A. Gupta, B. Mamindlapelly, P. L. Karuthedath, R. Chowdhury, and A. Chakrabarti. Adaptive isogeometric topology optimization using PHT splines. *Comput. Meth. Appl. Mech. Eng.*, 395:114993, 2022.
15. K. A. Johannessen, T. Kvamsdal, and T. Dokken. Isogeometric analysis using LR B-splines. *Comput. Meth. Appl. Mech. Eng.*, 269:471–514, 2014.
16. H. Kang, J. Xu, F. Chen, and J. Deng. A new basis for PHT-splines. *Graphical Models*, 82:149–159, 2015.
17. G. Kiss, C. Giannelli, U. Zore, B. Jüttler, D. Großmann, and J. Barner. Adaptive CAD model (re-) construction with THB-splines. *Graphical Models*, 76(5):273–288, 2014.
18. S. Kleiss, B. Jüttler, and W. Zulehner. Enhancing isogeometric analysis by a finite element-based local refinement strategy. *Comput. Meth. Appl. Mech. Eng.*, 213-216:168–182.
19. R. Kraft. *Adaptive und linear unabhängige Multilevel B-Splines und ihre Anwendungen*. PhD thesis, Universität Stuttgart, 1998.
20. X. Li, J. Zheng, T. W. Sederberg, T. J. Hughes, and M. A. Scott. On linear independence of T-spline blending functions. *Comput. Aided Geom. Des.*, 29(1):63–76, 2012.
21. A. Mantzaflaris. An overview of Geometry plus Simulation modules. In *Mathematical Aspects of Computer and Information Sciences. MACIS 2019*, volume 11989 of LNCS, pages 453–456. Springer, 2020.
22. Q. Ni, X. Wang, and J. Deng. Modified PHT-splines. *Comput. Aided Geom. Des.*, 73:37–53, 2019.
23. F. Patrizi and T. Dokken. Linear dependence of bivariate Minimal Support and Locally Refined B-splines over LR-meshes. *Comput. Aided Geom. Des.*, 77:101803, 2020.
24. F. Patrizi, C. Manni, F. Pelosi, and H. Speleers. Adaptive refinement with locally linearly independent LR B-splines: Theory and applications. *Comput. Meth. Appl. Mech. Eng.*, 369:113230, 2020.
25. T. W. Sederberg, J. Zheng, A. Bakenov, and A. Nasri. T-splines and T-NURCCs. *ACM Transactions on Graphics*, 22(3):477–484, 2003.
26. V. Skytt, O. Barrowclough, and T. Dokken. Locally refined spline surfaces for representation of terrain data. *Computers & Graphics*, 49:58–68, 2015.
27. A. Vuong, C. Giannelli, B. Jüttler, and B. Simeon. A hierarchical approach to adaptive local refinement in isogeometric analysis. *Comput. Meth. Appl. Mech. Eng.*, 200(49-52):3554–3567, 2011.
28. F. Weller and H. Hagen. Tensor product spline spaces with knot segments. In M. Dæhlen, T. Lyche, and L. Schumaker, editors, *Mathematical Methods for Curves and Surfaces*, pages 563–572. Vanderbilt University Press, Nashville, 1995.
29. H. Yang and C. Dong. Adaptive extended isogeometric analysis based on PHT-splines for thin cracked plates and shells with Kirchhoff–Love theory. *Applied Mathematical Modelling*, 76:759–799, 2019.
30. Y. Zhu and F. Chen. Modified bases of PHT-splines. *Commun. Math. Stat.*, 5(4):381–397, 2017.